ELSEVIER

J. Non-Newtonian Fluid Mech. 148 (2008) 97–108

Journal of Non-Newtonian Fluid Mechanics

www.elsevier.com/locate/jnnfm

# Filament stretching rheometry and break-up behaviour of low viscosity polymer solutions and inkjet fluids

T.R. Tuladhar, M.R. Mackley *

*Department of Chemical Engineering, University of Cambridge, Cambridge CB2 3RA, UK*

**Abstract**

This paper reports experimental observations on the way certain low viscosity Newtonian, polymer and inkjet fluids respond to filament stretching experiments that have been carried out using a variant of a multipass rheometer (MPR). A series of experiments were conducted where the opposing pistons of an MPR were used to provide controlled separation of two flat surfaces. Using 1.2 and 5.0 mm diameter pistons, a small quantity of test fluid was positioned between the pistons and the two pistons were moved apart at an equal and opposite velocity, thereby enabling optical interrogation of the central position of the filament that formed between the pistons faces. High speed photography followed the way the resulting fluid filament stretched and relaxed when the pistons movement had stopped. Different piston diameters, piston velocities and final piston separation were explored and the filament stretching and break-up was classified into regimes of behaviour. Approximate extensional viscosity parameters were obtained from the results. In some cases it was possible to correlate the filament stretching behaviour with the inkjet printing behaviour of a particular fluid.


*Keywords:* Filament stretching; Filament thinning; Low viscosity fluids; Inkjet fluids; Extensional viscosity

## 1. Introduction

Inkjet printers operate by ejecting a series of droplets of ink from nozzles onto a substrate and an important element of inkjet printing performance is the ink composition and physical properties such as viscosity, viscoelasticity, surface tension and inertia (see for example de Gans et al. [1]). When the ink exits a nozzle, a progressive necking and break-up of the jet occurs downstream of the nozzle. Controlling droplet formation and in particular, the formation and break-up of filament of the ink is a complex process that depends on many factors including the rheology of the ink [2]. Viscosity and elastic stresses resist the necking motion of the liquid filament and surface tension and inertia also influence the resulting shape and form of the emerging drop [1,3,4]. The viscosity of the ink should be suitably low, and typically 20 mPa s [1] in order to minimise pressure drop within the small diameter nozzle and also to facilitate subsequent deposition of the drop on a substrate.

Ink formulators often encounter problems where slight alterations in ink composition cause inconsistency in jet performances and print quality even though the formulation and physical properties are normally similar (personal communication with members of the Cambridge Inkjet Consortium). Predicting the reliability of the ink in terms of its base physical properties such as viscosity and surface tension alone is difficult as there are many intrinsic physical and chemical properties that contribute the overall reliability of the ink. Apart from the ink's physical properties, consistency of jet velocity through the nozzle, exit contact conditions of the ink leaving the nozzle and the transient driving pressure of the flow are also important [2]. Formulating inkjet inks in conjunction with a particular print head is often currently achieved by trial and error by varying the composition of the ink to produce reliable print quality. In this paper filament stretching techniques are used to access inkjet rheology and performance as many aspects of filament stretching have similar characteristics with the mechanics of inkjet drop formation.

Filament stretching techniques have been employed since the early 1990s to investigate the visco-capillary thinning of slender filaments that have a distinctive dependence on time and material properties (see for example, review paper by McKinley [4]). In terms of recent developments, Bazilevsky et al. [5]

* Corresponding author. Tel.: +44 1223 334777; fax: +44 1223 334796.
*E-mail addresses:* trt21@cam.ac.uk (T.R. Tuladhar), mrm1@cheng.cam.ac.uk (M.R. Mackley).

0377-0257/$ – see front matter © 2007 Elsevier B.V. All rights reserved.
doi:10.1016/j.jnnfm.2007.04.015

**Nomenclature**

| | |
|---|---|
| Bo | Bond number ($\rho g R^2/\sigma$) |
| $D$ | filament diameter (m) |
| $D_0$ | filament diameter just after stretching at $t=0$ (m) |
| $D_i$ | initial sample diameter (m) |
| $D_{mid}$ | mid-filament diameter (m) |
| $g$ | gravity (m/s$^2$) |
| $G'$ | elastic modulus (Pa) |
| $G''$ | viscous modulus (Pa) |
| $h_0$ | initial sample height (m) |
| $h_f$ | stretched sample height (m) |
| Oh | Ohnesorge number ($\eta_0/\sqrt{\rho\sigma R_0}$) |
| $R$ | filament radius (m) |
| $R_0$ | filament radius just after stretching at $t=0$ (m) |
| $t$ | time (s) |
| $t_b$ | filament break-up time (s) |
| Tr | Trouton ratio ($\eta_E/\eta_o$) |
| $v_p$ | initial stretch velocity (m/s) |
| $X$ | correction term in Eq. (5) |

*Greek letters*

| | |
|---|---|
| $\dot{\varepsilon}$ | strain rate (s$^{-1}$) |
| $\eta_0$ | zero shear viscosity (Pa s) |
| $\eta_E$ | extensional viscosity (Pa s) |
| $\eta_S$ | solvent viscosity (Pa s) |
| $\rho$ | fluid density (kg/m$^3$) |
| $\sigma$ | surface tension (N/m) |
| $\Delta\tau_P$ | polymeric tensile stress difference (Pa) |

invented an original design of a liquid filament rheometer (LFR) where the technique involved placing a drop of fluid between two plates and rapidly displacing the top plate to a set displacement by a spring mechanism. The extension produces a liquid filament between the two plates and the shape of the thinning filament was then either measured or observed optically until break-up. Several other variants of LFR have subsequently been developed. Kolte and Szabo [6] used a device where the plates are no longer separated by a spring mechanism and instead the bottom plate is lowered under gravity to a preset displacement by an air brake to produce a filament. Based on the pioneering work of Bazilevsky group's LFR, Cambridge polymer group (Cambridge, USA) have developed a commercial version of capillary break-up extensional rheometer (CaBER$^{TM}$—designed and manufactured by Thermo Electron). The apparatus operates using a laser micrometer to follow filament diameter evolution. The LFR provides a simple way of extracting the surface tension and the extensional viscosity of Newtonian fluids, or alternatively the single relaxation time of viscoelastic fluids, by analysing the diameter variation of the fluid thread [7,8].

A first approximation simple theory can be developed to describe the thinning of the viscous filament between the two plates. The model assumes an axially uniform cylindrical filament of mid-point diameter, $D_{mid}(t)$, thinning under the action of capillary pressure. There is an internal pressure within the filament due to the curvature of the filament's cylindrical section and surface tension. Ignoring inertia, gravity and the axial curvature along the filament, this driving pressure forces fluid within the filament towards the base reservoir at each ends and is assumed to be in quasi-static equilibrium with the combined viscous and viscoelastic forces within the filament (see [4–6,8,9] for detailed analysis) giving:

$$3\eta_S\dot{\varepsilon} + \Delta\tau_P(t) = \frac{2\sigma}{D_{mid}(t)} \tag{1}$$

where $\eta_S$ is the solvent viscosity, $\dot{\varepsilon}$ the strain rate, $\sigma$ the surface tension and $\Delta\tau_P$ is the polymeric tensile stress difference. In this equation, the external longitudinal stress along the fluid thread is assumed to be zero at all times as the column is connected to quasi-static fluid reservoirs which are themselves attached to the rigid endplates of the device [10]. The strain rate, $\dot{\varepsilon}$, for a slender filament can be expressed in terms of the rate of evolution of filament diameter by [9]:

$$\dot{\varepsilon} = -2\frac{\mathrm{d}\,\ln(D_{mid}(t)/D_0)}{\mathrm{d}t} = -\frac{2}{D_{mid}(t)}\frac{\mathrm{d}D_{mid}(t)}{\mathrm{d}t} \tag{2}$$

A differential equation describing the transient evolution of the diameter can then be obtained by substituting Eq. (2) into (1) giving:

$$3\eta_S\left(-\frac{2}{D_{mid}(t)}\frac{\mathrm{d}D_{mid}(t)}{\mathrm{d}t}\right) + \Delta\tau_P = \frac{2\sigma}{D_{mid}(t)} \tag{3a}$$

For a Newtonian fluid Eq. (3a) becomes:

$$3\eta_S\left(-\frac{2}{D_{mid}(t)}\frac{\mathrm{d}D_{mid}(t)}{\mathrm{d}t}\right) = \frac{2\sigma}{D_{mid}(t)} \tag{3b}$$

Independent of the choice of a fluid constitutive equation, an apparent extensional viscosity, $\eta_E$, can be related to the mid-filament diameter by taking the ratio of the capillary pressure in the filament to the instantaneous strain rate in Eq. (1) [9] giving:

$$\eta_E(t) = 3\eta_S + \frac{\Delta\tau_{P(t)}}{\dot{\varepsilon}(t)} = \frac{\sigma}{(-\mathrm{d}D_{mid}(t)/\mathrm{d}t)} \tag{4}$$

Liang and Mackley [8] measured the filament thinning response of high viscosity solution using a LFR developed by the Bazilevsky's group. They reported (i) a linear thinning of high viscosity Newtonian (polydimethylsiloxane, PDMS) solution and (ii) an exponential decay of polymer (poly-*iso*-butylene, PIB) solution with time. Using an independent measurement of $\eta_S$, they extracted the surface tension value for PDMS from Eq. (3b) which was found to be approximately a factor of 2 below the reported literature value. Their data were further analysed by Entov and Hinch [7] who extended the theoretical analysis by considering the effect of multiple relaxation time modes and finite extensibility of polymer chains. Kolte and Szabo [6] investigated the capillary thinning of a Newtonian polybutene and a viscoelastic poly-*iso*-buytlene solution and also reported discrepancies between the theoretical prediction and experimental values of the mid-filament diameter. They concluded that the simple analysis was not sufficient to fully explain the observed capillary thinning behaviour. A recent review paper [4] extensively examines the capillary thinning and break-up behaviour

Table 1
Test fluids composition and physical properties

| | Series I polymer solutions | Series II DOD UV inks | Series III CIJ alcohol based inks |
|---|---|---|---|
| Solvent | Diethyl phthalate (DEP) | Monofunctional isobornyl acrylate (IBOA) | Ethanol |
| Viscoelasticity enhancer | PS | Multifunctional acrylate | PVP |
| Others | | UV agent dye | Conducting agent |
| Key variables | PS (0–5 wt%) | IBOA (75–85 wt%), multifunctional acrylates (0–25 wt%), UV agent (0–15 wt%) | PVP (0.7–14 wt%), PVP Mol wt. ($2 \times 10^3$–$1.5 \times 10^6$ g/mol) |
| $\eta_0$ at 25 °C (mPa s) | 10–90 | ∼23–24 | ∼3–5 |
| $\sigma$ (mN/m) | ∼37 | ∼32 | ∼25 |
| $\rho$ (kg/m$^{3)}$ | ∼1120 | ∼1040 | ∼800 |

of complex fluids and identifies Newtonian and non-Newtonian (Bingham plastic, power law, weakly elastic and elastic) fluids based on the qualitative profiles of liquid filament and distinctive temporal evolution of the mid-point filament diameter.

Work reported in this paper describes the filament thinning response of low viscosity Newtonian, polymer and inkjet fluids using a variant of a multipass rheometer (MPR). The MPR was developed by Mackley et al. [11] at the University of Cambridge and consists of two independently controlled top and bottom pistons. Piston displacement is controlled by servo-hydraulic movement. In a filament stretching mode of operation described here, an equal and opposite velocity signal was applied to each piston to regulate both piston displacement velocity and position. For a typical experiment, the pistons started with a spacing of 0.3–1.2 mm and finished with a separation of 1.3–5.0 mm, with pistons velocities ranging from 50 to 300 mm/s. A useful feature of the MPR is its capability to impose very rapid extensional deformations and thus form thin filaments from fluid with low viscosities. Other positive features of this experimental configuration include the independent control of both pistons, thus fixing the mid-filament position during the entire process. Relatively little filament stretch work has been published before on low viscosity systems where there are difficulties involving the necessity of high strain rates and fast relaxation processes (see for example [12]). Recently, Tirtaatmadja et al. [13] investigated the dynamics of drop formation and break-up of low viscosity polymeric fluids by ejecting the fluid out from a 2 mm nozzle using a syringe pump.

The MPR was also used in its conventional form to measure high shear rheology of the inks. Background to the general operation of the MPR is given in Mackley et al. [11]. The sample under test was constrained within a 'test section' that comprised of a capillary held between two barrels. The servo-hydraulically controlled pistons were located in two barrels (top and bottom sections), both of which were fitted with pressure transducers and thermocouples. The temperature of the sample was controlled by flowing heated silicon oil from a heater/circulator through the heated jackets around the bottom and top barrels and the test section. The sample under study could be driven back and forth through a capillary test-section by hydraulic pistons, hence the name multipass rheometer (MPR). This unique arrangement allows rheological experiments to be carried out on small sample volume (<15 g), multi-phase system and at high pressure. In this study, the MPR was used in a more standard way, in a single pass mode, where the sample was driven only in one direction in a similar fashion to a conventional capillary rheometer.

## 2. Test fluids

Three formulations were investigated as shown in Table 1. In the first series, a laboratory formulated range of polystyrene solutions were prepared in order that the systematic effect of polymer concentration could be followed. A range of four diethyl phthalate (DEP) and polystyrene (PS) solutions were formulated in the laboratory with varying PS concentration (0, 1.0, 2.5 and 5.0 wt%) to investigate the effect of polymer concentrations on rheology and filament profiles. The 99.5% purity DEP was obtained from Sigma–Aldrich (Product no: 524972) and the linear polystyrene with weight average molecular weight of 195,000 g/mol (polystyrol VPT granule) was supplied by BASF. The 5.0 wt% DEP-PS solution was prepared by dissolving PS in DEP solvent at 130 °C and constant stirring for 10 h. Other solutions were prepared by dilution of the original 5.0 wt% solution to the required concentration. Table 2 lists the detailed compositions and other properties of the PS-DEP solutions.

A second series of experiments were carried out using drop on demand (DOD) inks. The second tests were carried out on four variants of UV inks supplied by SunJet (http://www.sunchemical.com/sunjet/) with varying compositions of acrylate and UV agents while retaining similar viscosity (∼24 mPa s) and surface tension (∼32 mN/m) at 25 °C.

Finally, a third series of experiments were carried out for continuous inkjet (CIJ) formulation. This series consisted of five variants of alcohol (ethanol) based CIJ ink containing different molecular weights of polyvinyl-pyrrolidone (PVP) whilst

Table 2
PS concentration and other properties of Series I DEP-PS solutions

| DEP solution | PS concentration (wt%) | $\eta_0$ at 25 °C (mPa s) | Oh at $t = 0$ of Fig. 3 | Oh at $t = 0$ of Fig. 6 |
|---|---|---|---|---|
| DEP0 | 0.0 | 10 | 0.10 | 0.05 |
| DEP1 | 1.0 | 15 | 0.15 | 0.08 |
| DEP2 | 2.5 | 33 | 0.35 | 0.17 |
| DEP3 | 5.0 | 90 | 0.92 | 0.46 |

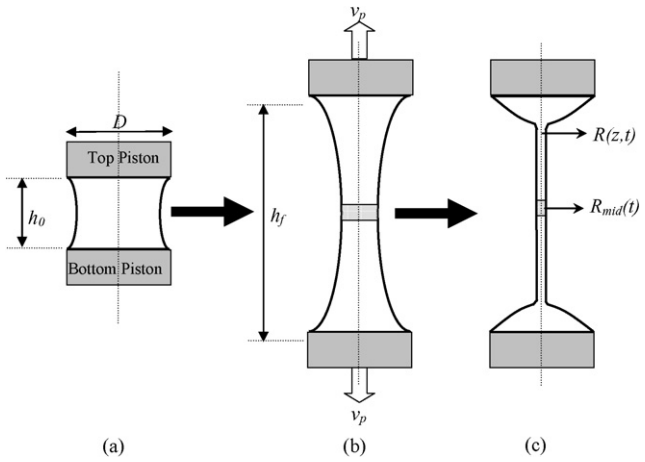


Fig. 1. Schematic diagram of MPR filament stretching and thinning experiment. (a) Test fluid positioned between two pistons. (b) Test fluid stretched uniaxially at a uniform velocity $t < 0$. (c) Filament thinning and break-up occurrence after pistons has stopped $t \geq 0$.

retaining similar viscosity (~3–5 mPa s) and surface tension (~25 mN/m) at 25 °C. The inks were supplied by Domino (www.domino.com).

## 3. Experimental protocol

The basic configuration of the MPR filament stretching rheometry is shown schematically in Fig. 1. A small volume of test fluid of initial height, $h_0$, was positioned between the top and bottom pistons of specified diameter (1.2 and 5 mm used here). Both pistons were then moved away from each other to a set displacement ($h_f$) at a constant velocity, $v_p$. As a result of rapid initial axial stretching, the fluid filament of near central uniform thickness was formed. This filament then thinned under the combined action of surface tension, inertia and rheological effects. Optical interrogation of the filament constrained axially between the two pistons during and after stretching was observed using a high speed camera (Kodak motion corder analyzer, SR-c series) with a Leica zoom seven lens at 1000 frames per second. Each image is 256 × 240 pixel resulting in the image resolution of ca. 6 μm (for 1.2 mm piston) and 21 μm (for 5.0 mm pistons) per pixel. A positive feature of this experimental configuration is the independent control of both top and bottom pistons, thus fixing the mid-filament position during the entire process. Each piston could be moved over a wide range of velocities from 1 to 300 mm/s and a maximum displacement of 30 mm on each side. The filament stretching experiments were performed at room temperature.

## 4. Experimental observations and discussion

### 4.1. Series I fluids: DEP-PS solutions

#### 4.1.1. Rheo measurements

Fig. 2 shows simple shear viscosity data for the Series I, DEP-PS solution fluids at both low and high shear rate. The low shear rate data were obtained using a controlled strain parallel plate rheometer (Rheometrics ARES) and the high shear data using an MPR in a single pass mode. The DEP solvent alone is Newtonian and the addition of PS results in some shear thinning behaviour of the solution. At 1.0 wt% PS, there was little change in the viscosity over a wide range of shear rates (10–$10^5$ $s^{-1}$) and appeared fairly Newtonian. With a further increase in PS concentration (2.5 and 5.0 wt%), the fluid viscosity showed a classic shear thinning behaviour.

Dynamic oscillatory experiments were carried out to explore the effect of viscoelasticity using the ARES rheometer. In the range of frequencies (1–100 rad/s) studied, the viscous component ($G''$) was always dominant over the elastic component ($G'$) for all DEP-PS solution. The $G'$ was negligible at low frequencies. Unfortunately high frequency viscoelastic properties for these solutions could not be obtained using standard oscillatory rheometers and so the high frequency viscoelastic of the test fluid was not established.

#### 4.1.2. Filament stretch observation of DEP-PS solutions

A series of MPR filament stretching experiments were carried out to observe the way in which low viscosity filament profiles thinned. If low stretching velocities were used, the filaments broke during stretching before they reached a final position. This was overcome by rapidly stretching the sample at high piston velocities ($v_p > 80$ mm/s) such that an intact filament formed, allowing filament relaxation and thinning to be observed after the piston stopped moving.

Fig. 3 shows a sequence of video images for MPR filament stretching, thinning and break-up for the Newtonian DEP solvent and DEP-PS solutions at 25 °C using 1.2 mm piston diameter. Here, each sample with initial diameter $D_i$ (~1.2 mm) and height $h_0$ (~0.35 mm) was rapidly stretched to a final height $h_f$ (~1.35 mm) by moving each piston 0.5 mm apart at 200 mm/s. This resulted in an initial sample aspect ratio ($D_i/h_0$) and a stretch ratio ($h_f/h_0$) of 3.4 and 3.9, respectively. The first image at $t = -2.5$ ms corresponds to the initial configuration of the liquid bridge where the fluid appeared almost cylindrical. For all cases, the cylindrical filament deformed into an unstable necked configuration but remained axisymmetric about the mid-filament plane during and after stretching thereby indicating negligi-

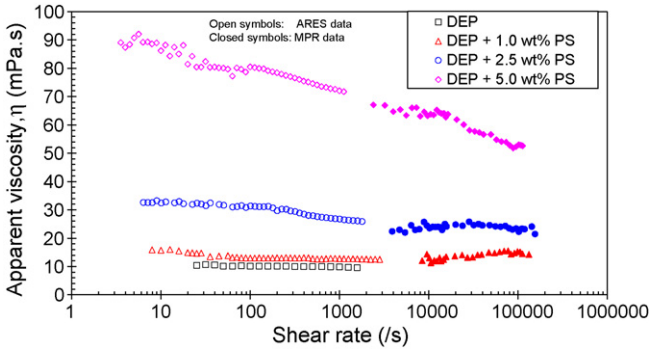


Fig. 2. Effect of PS concentration on the apparent shear viscosity of DEP solvent and DEP-PS solutions for a range of shear rates at 25 °C using (a) ARES parallel plate configuration for low shear rates (open symbols) and (b) MPR for high shear rates experiments (closed symbols).

ble gravity effect. This can also be validated from calculation of the Bond number, Bo, (the ratio of gravity to surface tension force = $\rho g R^2/\sigma$) which was significantly less than 1 for all cases. The images following the cessation of stretching ($t > 0$) showed progressive filament thinning and formed various complex filament shapes leading to final break-up. The emergence of complex filament shapes (rather than cylindrical) during the relaxation could result from the influence of inertia, surface tension and rheological stresses [14,15].

Qualitative observation of the figures showed significant variation in the way filament thinned with a change in PS concentration. Fig. 3(a) shows the filament thinning profile for a low viscosity Newtonian DEP solvent (DEP0). In this case, the axial profile of the filament was non-uniform and rapidly thinned by

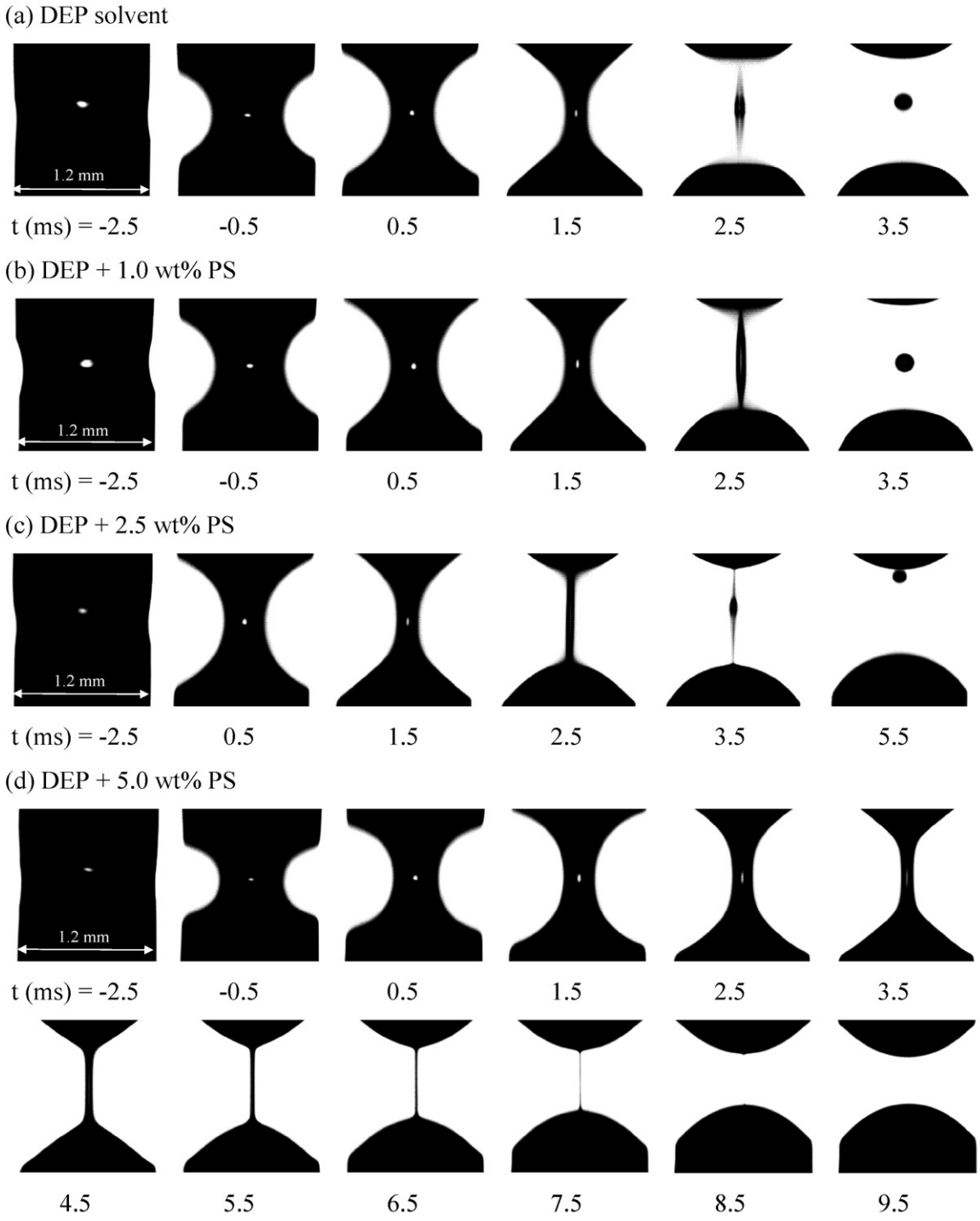


Fig. 3. Sequence of high speed video images showing filament stretching, thinning and break-up of Series I, DEP solvent and DEP-PS solutions, (the piston diameter in all sequence is 1.2 mm). Initial sample height of approximately 0.35 mm fluid is stretched to 1.35 mm by moving each piston 0.5 mm apart at a constant velocity of 200 mm/s.

"end pinching" at both ends of the filament which resulted in the formation of a central drop. This behaviour contrasts with that of high viscosity Newtonian fluids observed by others [8,9]. They reported break-up occurring close to the mid part of the filament with no drop formation. The addition of a low concentration of PS in DEP solvent (DEP1) did not change the filament thinning profile as shown in Fig. 3(b); however, with a further increase in PS concentration (DEP2 and 3), the filament became more uniformly cylindrical and stable at the later stages of thinning (see for example Figs. 3(c) and (d)). For the 5.0 wt% PS solution (DEP3), the filament diameter was essentially uniform along the whole length of the filament throughout the thinning process and connected to the two approximate hemispherical fluid reservoirs attached to each piston. For the high PS concentration solution, the filament finally broke at the mid-filament position instead of end pinching. After the filament had broken at the central region, capillary action pulled the broken filament towards the fluid reservoir on each piston, resulting in two fluid reservoirs and no independent drop formation. A filament break-up time, $t_b$, can be obtained from the data and yields a value of 3.5 ms for the DEP solvent and a maximum value of 8.5 ms for the high PS concentration DEP3 solution. Error in measurement of $t_b$ is of order 1 ms.

Fig. 4(a) shows quantitative analysis of Fig. 3, where the mid-filament diameter is plotted against time, during and after stretching. The normalised filament diameter of the thinning process after the cessation of piston movement is shown in Fig. 4(b). The filament diameter of Newtonian DEP solvent, DEP1 and DEP2 decreased rapidly with time. For the Newtonian fluids, the filament is predicted to thin linearly with time [4–8]. However, the precise decay profile during capillary thinning could not be fully obtained for these solutions due to rapid break-up of the filaments after stretching. The higher concentration PS solution (DEP3) exhibited a different behaviour where the filament diameter decreased exponentially with time. This exponential decay profile probably originates from an initial Newtonian response of the solvent followed by PS viscoelasticity dominance at the later stage. Experiments on high viscosity polymer solutions (>1 Pa s) have shown similar exponential decay profiles during the thinning processes [4–6,8].

Additional filament stretching experiments were carried out to determine whether the initial stretch velocity ($v_p$) had an influence on the subsequent thinning process. Fig. 4(c) examines

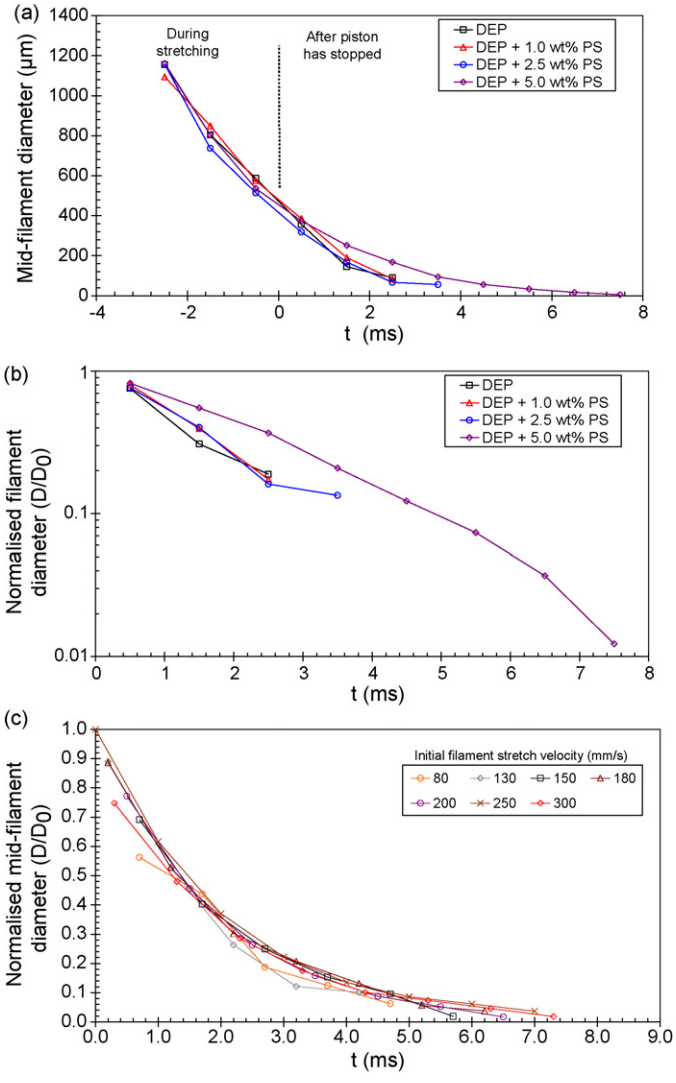


Fig. 4. Mid-filament diameter profiles of Fig. 3. (a) Filament profiles during stretching and thinning of Series I, DEP-PS solutions; (b) Normalised filament thinning profile after the piston has stopped in semi-log plot. (c). Effect of initial filament stretch velocity on filament thinning profile of Series I, DEP and 5.0 wt% PS after the piston has stopped. The piston diameter in all sequence is 1.2 mm. Initial sample height of approximately 0.2 mm fluid is stretched to 1.2 mm by moving each piston 0.5 mm apart at a constant velocity.

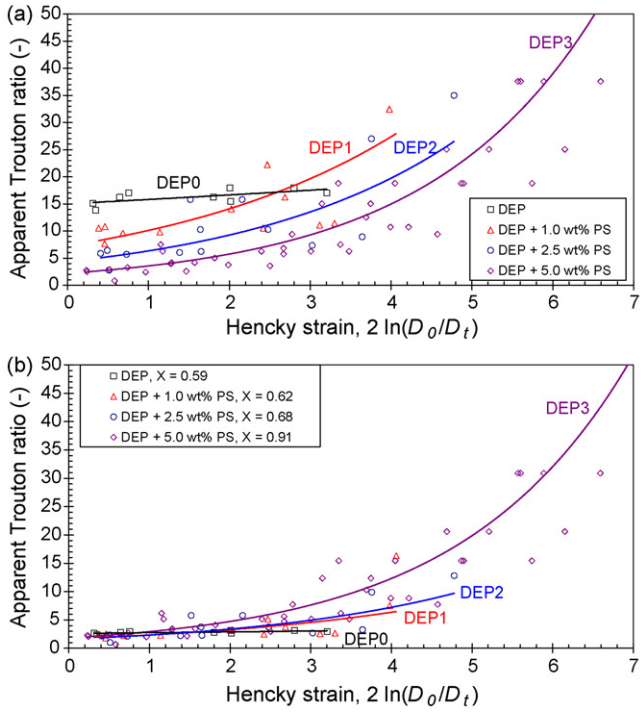


Fig. 5. (a) The transient extensional rheology of DEP-PS solutions as a function relaxation Hencky strain. $D_t$ is the diameter of the filament at the mid point between the pistons. The solid lines represent fitting trendlines. (b). The transient extensional rheology of DEP and PS solution by incorporating correction term, $X$. The solid lines represent fitting trendlines.

the filament thinning of DEP3 during relaxation after the initial stretch at various piston speeds. The figure shows that $v_p$ has little effect on the filament thinning profile. All the filaments exhibited similar exponential decay profiles.

Further analysis on the filament thinning was carried out using Eq. (4) and the results for apparent Trouton ratio ($Tr = \eta_E/\eta_o$) presented in Fig. 5. Eq. (4) assumes an axially uniform cylindrical filament and neglects the effect of inertia, gravity and the axial curvature. Fig. 5(a) shows a plot of apparent Tr as a function of the total relaxation Hencky strain ($=2\ln(D_0/D_t)$) after the piston has stopped. Here, a series of experiments were carried out over a range of initial piston speeds $v_p$ (80–300 mm/s) with similar initial aspect and stretch ratio including results from Fig. 4. The mid-filament data obtained in the early stages and from axially uniform cylindrical shapes are only considered. Data close to the break-up stages have not been included. Only a few data points were obtained for low viscosity DEP solvent and DEP1 as the filament broke quickly after the pistons stopped. For a Newtonian solution, the Tr should be 3 and independent of strain. Although the Tr was uniform for low viscosity DEP solvent, its value was much greater than 3 as predicted for Newtonian

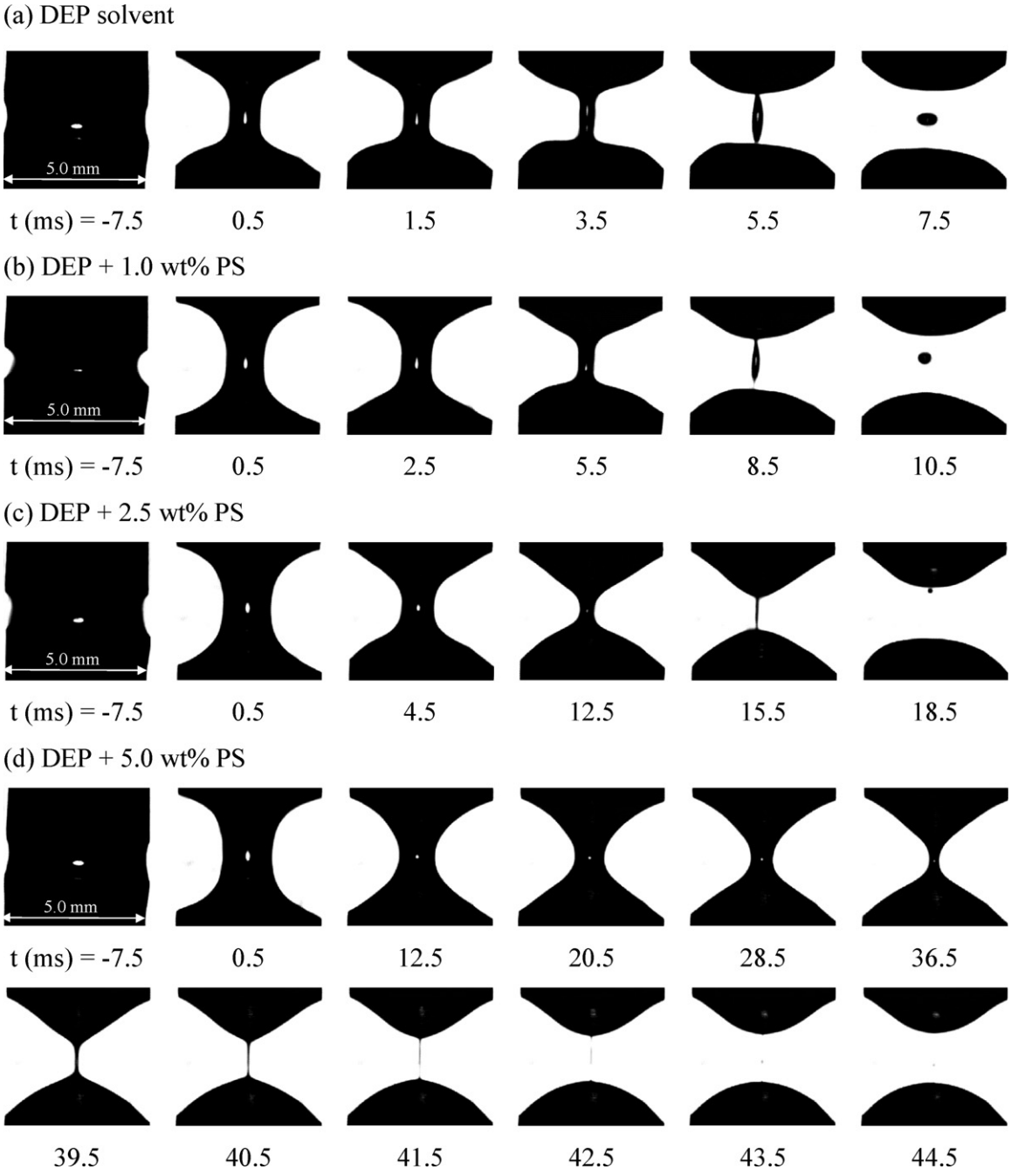


Fig. 6. Sequence of high speed video images showing filament stretching, thinning and break-up of DEP-PS solutions (the piston diameter in all sequence is 5.0 mm). Initial sample height of approximately 1.2 mm fluid is stretched to 4.2 mm by moving each piston 1.5 mm apart at a constant velocity of 200 mm/s.

fluid. This discrepancy can result from neglecting the effect of axial curvature and inertia in Eq. (4) as the filament profile for these experiments deviated significantly from a uniform cylinder required for the simple analytical model (Eq. (4)). In terms of inertial effect, the values of the Ohnesorge number, Oh, (ratio of viscous to surface tension force $= \eta_0/\sqrt{\rho\sigma R_0}$) for the DEP-PS solutions are given in Table 2 and show that for low PS concentration (DEP0–DEP2), the Oh values are less than 1 indicating considerable contribution of inertia. With increasing PS concentration, the Tr decreased and approached close to 3 (at lower strain) corresponding to the filament shape becoming more cylindrical and diminishing inertial effect. For DEP3, the Tr started in the order of 3.0 and then steadily climbed up at later stages (high strain) due to significant extension of polymer molecules. This diminishing inertial effect is also represented in the Oh which was close to 1 at $t = 0$.

The discrepancies in the viscosity obtained from the experimental data when using the simple analysis (Eqs. (3a), (3b) and (4)) have also been reported in the literature and time-dependent numerical simulations of the evolution of the filament showed the additional importance of both gravity [6,10] and inertia [16–18]. McKinley and Tripathi [10] introduced an $X$ factor correction in the simple model to accurately analyse the thinning of a mid-filament diameter of a Newtonian liquid. We have also introduced this adjustable $X$ correction term in Eq. (4) to account for the $\eta_E$ discrepancy giving

$$\eta_E(t) = (2X - 1)\frac{\sigma}{(-\mathrm{d}D_{mid}(t)/\mathrm{d}t)} \quad (5)$$

where $X$ takes account of the effect of double curvature, inertia and gravity. The equation is equivalent to Eq. (4) when $X$ equal is to 1. McKinley and Tripathi [10] reported that numerical simulations by others [16–18] determined $X$ to be between 0.53 and 0.71 for inertia and inertia-less Newtonian viscous cylindrical filaments respectively. They also showed experimentally that the most appropriate value of $X$ was 0.7127 for typical viscous Newtonian fluid filaments such as glycerol and silicone oil. The $X$ factor becomes relevant when certain dimensionless groups such as Oh falls below unity or Bo exceeds unity. The Oh $\leq 1$ establishes the relative importance of inertia and hence curvature [4] and the Bo $\geq 1$ gives the importance of gravity [9]. For the experiments described in this paper, the Oh and Bo numbers at $t = 0$ ranged from 0.1–0.9 to 0.0–0.3, respectively.

Fig. 5(b) shows the apparent Trouton ratio as a function of Hencky strain by fitting a value of $X$ in Eq. (5) for each DEP-PS solution. The most appropriate value of $X$ (shown in the figure legend) was obtained from the best fit of the initial linear filament thinning profile of Fig. 4(b). The value of $X$ for the Newtonian DEP solvent ($X = 0.59$) lies within the range reported in the literature for the Newtonian fluid and shows a uniform Tr of 3. With increasing PS concentration, the value of $X$ increased and approached closer to 1 for DEP3, suggesting diminishing curvature and inertial effect with increasing viscoelasticity. Eggers [18,19] showed numerically that, in the very final stages of break-up, inertial effects can no longer be neglected.

In order to increase filament break-up time, $t_b$, filament stretching experiments were also performed using a piston diameter of 5.0 mm with an initial sample height of 1.2 mm and a displacement of 1.5 mm on each side giving a final height of 4.2 mm. A stretch velocity of 200 mm/s was again used. The net effect of these changes was the ability to capture more data points. This resulted in an extra volume of ink being stretched, whilst maintaining a comparable $D_i/h_0$ (~4.1) and $h_f/h_0$ (~3.5) to that of Fig. 3. The video images (Fig. 6) of the filaments just after the pistons stopped ($t = 0$) are biconcave for all cases and were almost symmetrical about the mid-filament plane. Qualitatively, the filament profile obtained from these sets of experiments (Fig. 6) showed a similar behaviour to Fig. 3, where the shape of the liquid filament between the stagnant fluid reservoirs on each piston changed from biconcave at $t = 0$ to biconvex for low PS concentration (DEP1) and cylindrical shape with no drop for higher PS concentration solutions (DEP2–3) at later times. Quantitative analysis (Fig. 7) of the mid-filament diameter showed a linear decay with time for DEP solvent and low concentration PS solution (DEP1) confirming the Newtonian behaviour from the rheological tests (Fig. 2). Even for high PS concentration (DEP2 and DEP3), filament diameter appeared to decrease linearly for most of the time. The rate of decay, however, was slower for these solutions and the 5.0 wt% PS solution (DEP3) took much longer time to thin. An anticipated exponential final decay (similar to that observed when using small diameter piston, Fig. 4(b)) was not apparently visible. This could be due to our inability to detect small changes in filament diameter precisely towards the end (where the PS contribution would be influential) because of low image resolution for this setting (21 μm per pixel as compared to 6 μm for 1.2 mm piston setting). The Oh values were also less than 1 (Table 2) indicating the dominance of inertia for all these fluids at this test condition.

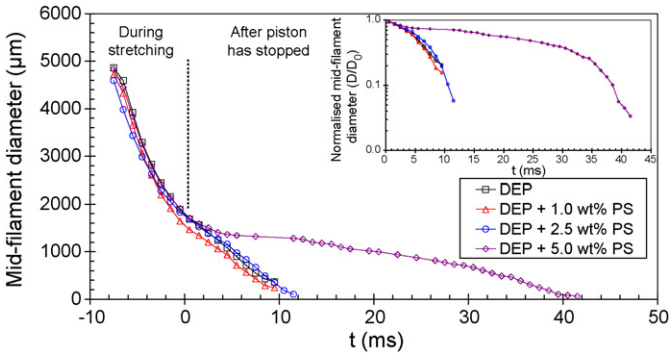


Fig. 7. Mid-filament diameter profiles during stretching and thinning of DEP-PS solutions of Fig. 6 (inset: normalised filament diameter after the piston has stopped in semi-log plot).

### 4.2. Series II fluids: UV inks

Four variants of UV ink were used to investigate whether a change in the composition of mono and multi-functional acrylate and UV agent altered the filament thinning and the printing behaviour in the inkjet print head. Steady shear rheology on these inks showed no or little simple shear dependency at 25 °C and were Newtonian over a wide range of shear rates (10–$10^5$ $s^{-1}$). The viscosity of all these UV inks were around 23–24 mPa s.

Dynamic tests, carried out over a wide range of frequencies (0–100 rad/s), showed very little or negligible elasticity ($G'$). Both steady and frequency tests did not distinguish any difference between these UV inks.

Fig. 8(a) shows a sequence of high speed video images for one of the UV ink using 5 mm piston diameter with operating conditions similar to Fig. 6. The filament shapes looked similar to that of Fig. 6(a) and (b) changing from biconcave at $t = 0$ to biconvex at later times indicating Newtonian behaviour. Fig. 8(b) shows the filament diameter profiles at three axial locations (mid position; top and bottom extreme ends). Initially the filament diameter decreased uniformly along the axial plane (for $t \leq 3$ ms), however, the filament thinned faster at the extreme axial ends (nearer the stagnant fluid reservoirs) than the mid-plane leading to biconvex profile at later times. Both qualitative and quantitative investigations on other UV inks did not show any significant changes in the filament thinning and break-up profiles. Filament stretching and thinning experiments for all these inks showed essentially Newtonian behaviour where the filament thinned linearly with time (except towards the end).

A further series of experiments were also carried out for all four UV inks over a range of $v_p$ (50–300 mm/s) and the data

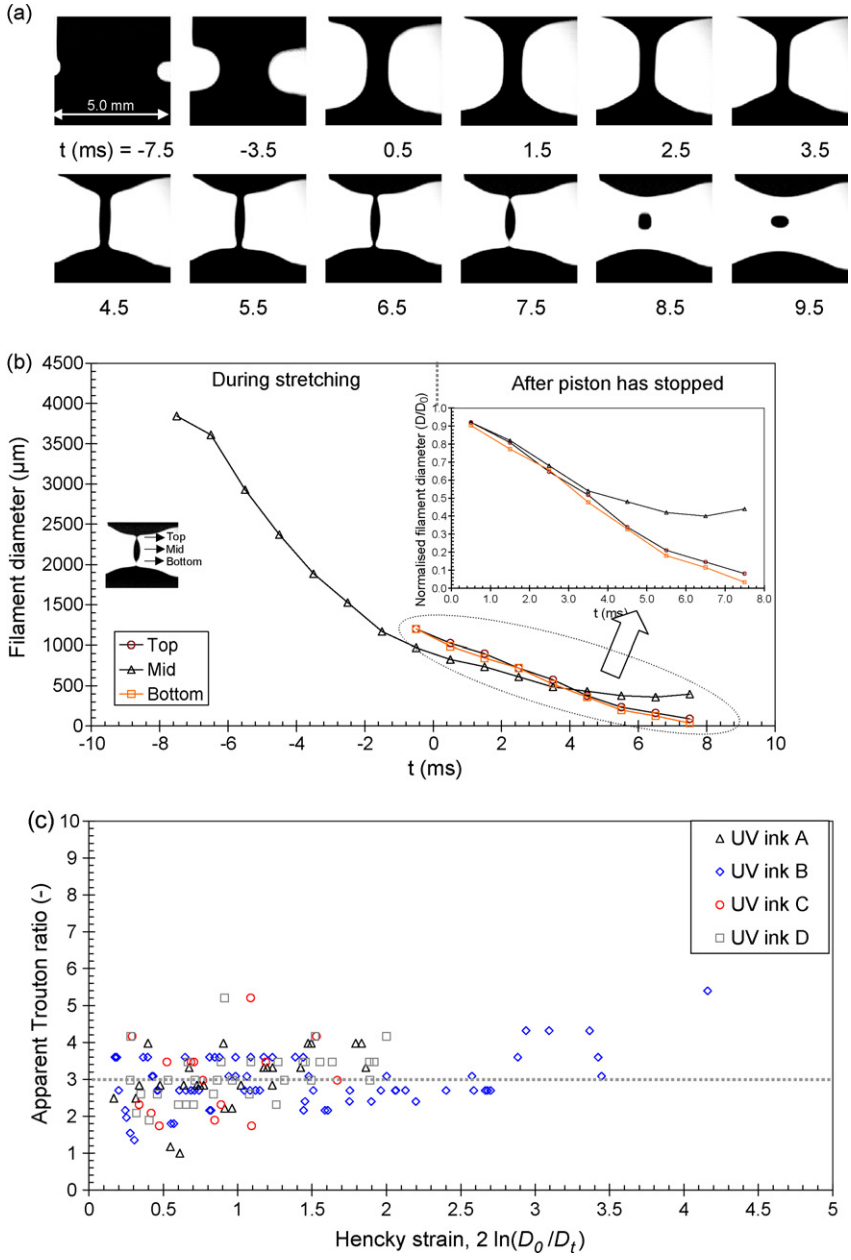


Fig. 8. (a) Sequence of high speed video images showing filament stretching, thinning and break-up of Series II Newtonian UV ink A (the piston diameter in all sequence is 5.0 mm). Initial sample height of approximately 0.52 mm fluid is stretched to 3.52 mm by moving each piston 1.5 mm apart at a constant velocity of 200 mm/s. (b). Filament diameter profiles of Series II UV ink A of Fig. 8(a) during stretching and thinning at 3 axial positions (Inset: normalised filament diameter after the cessation of piston movement). (c). The transient extensional rheology of UV ink from filament thinning profiles for four UV inks of similar physical properties incorporating correction term, $X = 0.63$–$0.64$.

from the early stages of the thinning profile are only incorporated where the filament thinned uniformly to calculate $\eta_E$. Fig. 8(c) shows the apparent Trouton ratio of these UV inks as a function of relaxation Hencky strain. Similar to the low viscosity DEP solvent, $X$ needs to be incorporated to accurately predict the filament thinning behaviour of such low viscosity inks. The $X$ value of 0.63–0.64 for all these inks gave the apparent Tr of around 3 indicating similar curvature and inertia effect for varying ink compositions and were also independent of strain. The behaviour of these inks in the DOD inkjet printer (work carried out at "The Cambridge Inkjet Research Centre", Cambridge, UK) also showed no significant change in the way jets and droplets formed as they exited the printer nozzle.

### 4.3. Series III fluids: CIJ inks

Further filament stretching experiments were carried out on five ethanol-based inks. The detailed compositions of the ink are listed in Table 3. Steady shear and frequency tests did not distinguish any differences between these CIJ inks and the fluids appeared Newtonian over a wide range of shear rates although they had varying concentration and molecular weight of polyvinylpyrrolidone (PVP). The viscosity of these inks were between 3 and 5 mPa s.

#### 4.3.1. Filament stretching and thinning

Fig. 9(a) shows the filament profiles during and after stretching for these CIJ inks using 1.2 mm piston diameter with experimental conditions similar to Fig. 3. The normalised filament diameter of the thinning process after the cessation of piston movement is shown in the inset. The axially non-uniform filament diameter decreased rapidly soon after stretching, followed by end pinching and formed a drop for low molecular weight inks (A–D). Ink E exhibited a different behaviour where the cylindrical filament thinned exponentially. The filament break-up time ($t_b$) for ink E was also longer than for other inks, although they had similar viscosities indicating marked elastic effect. The high molecular weight PVP possible influenced the decay, thereby delaying the necked fluid from breaking off.

Fig. 9(b) shows the apparent Trouton ratio as a function of relaxation Hencky strain from the filament profiles of Fig. 9(a) after the pistons had stopped. The $X$ value of 0.53 gave the apparent Tr of order 3 for the early stages of thinning for all inks. The Tr increased rapidly at later stages for ink E corresponding apparently to the stretching of the long chain PVP polymer. Though the influence of inertia is significant for all these low viscosity inks as illustrated by small $X$ (~0.53) and Oh (~0 as shown in

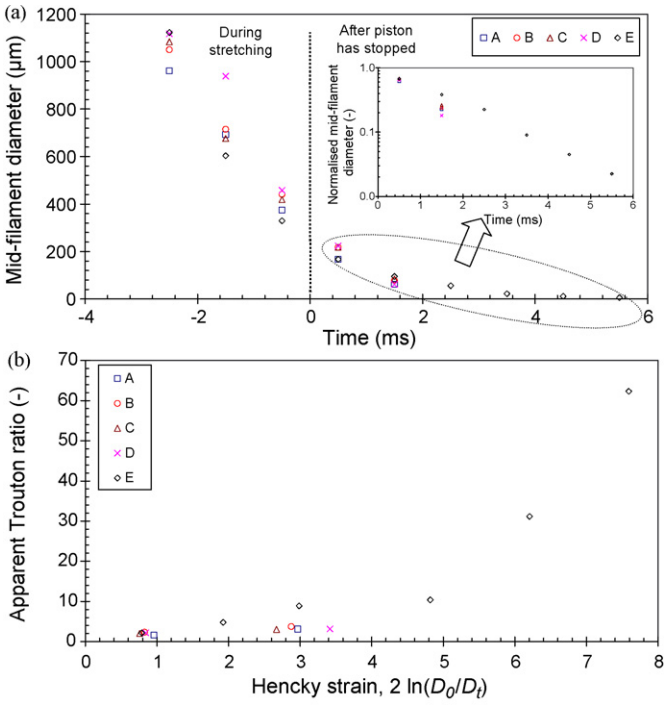


Fig. 9. (a) Mid-filament diameter profiles during stretching and thinning of the CIJ inks (inset: normalised filament diameter after the cessation of piston movement in semi-log plot). Filament thinning conditions similar to that of Fig. 3. (b). The transient extensional rheology of CIJ inks from filament thinning profiles of Fig. 9(a) incorporating correction term, $X = 0.53$.

Table 3) values, the presence of high molecular weight PVP in ink E appears to offset the break-up process by increasing the extensional viscosity of the solution.

#### 4.3.2. Correlation of filament stretching with inkjet performance

An investigation was carried out to compare the performance of the CIJ inks in a real inkjet printer head with that of the filament stretching experiments. Evaluation of the inks in a real inkjet printer showed different jet behaviour (Fig. 10). For low and moderate PVP molecular weight (inks A–D), the filament broke at a short distance from the nozzle and formed a droplet with a tail attached. This tail later broke from the mother droplet to form a satellite drop. The high molecular weight PVP ink E, however formed a long filament that did not break to give any droplet within the experimental time scale of measurement. The bottom photographs in Fig. 10 show matching filament profiles observed just before the break-up (obtained from experiments of Fig. 9) where inks A–D formed end pinching (nearer the

Table 3
PVP molecular weight and concentration of Series III alcohol-based ink and their properties

| CIJ ink | PVP molecular wt (g/mol) | PVP concentration (wt%) | $\eta_0$ at 25 °C (mPa s) | Oh at $t = 0$ |
|---|---|---|---|---|
| A | $2.0 \times 10^3$ to $3.0 \times 10^3$ | 14.0 | 4.9 | 0.09 |
| B | $7.0 \times 10^3$ to $1.1 \times 10^4$ | 12.8 | 3.1 | 0.05 |
| C | $2.8 \times 10^4$ to $3.4 \times 10^4$ | 7.0 | 3.9 | 0.07 |
| D | $4.4 \times 10^4$ to $5.4 \times 10^4$ | 4.8 | 3.1 | 0.05 |
| E | $1.0 \times 10^6$ to $1.5 \times 10^6$ | 0.7 | 4.5 | 0.09 |

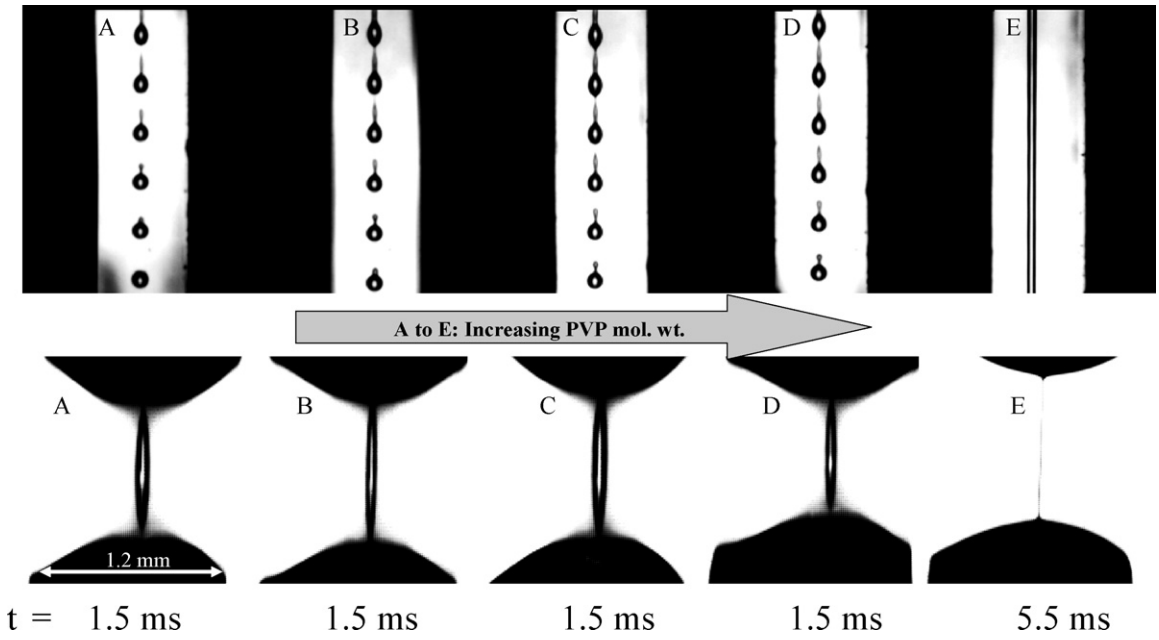


Fig. 10. Comparison of the inkjet printing behaviour of a Series III alcohol-based CIJ ink of varying PVP molecular weight with the filament stretching experiments. Top photographs show droplet formation from Linx CIJ inkjet printer head (Courtesy: Linx) and the bottom photographs show the filament profile just before the break-up.

fluid reservoirs) followed by a droplet formation. Ink E, however formed an axially uniform cylindrical filament during the thinning process and finally broke at the mid-plane. The broken filaments contracted to the connecting reservoirs on each piston, resulting in no droplet formation. These results suggest that the filament thinning and break-up experiments can be closely related to the actual process of inkjet printing involving filament formation and drop break-up and can be used to characterise the extensional rheology of complex fluids. An "ideal" ink would have a composition somewhere between D and E, where a clean filament break would occur without the formation of a satellite drop.

## 5. Conclusions

The simple shear rheology of inkjet fluids reported here demonstrates that these fluids remain essentially Newtonian in simple shear even at the shear rates experienced within inkjet printers. The high viscosity model DEP–PS solutions did however exhibit some shear thinning at high shear rates.

Transient filament stretching experiments of low viscosity fluids have been achieved using a modification to an MPR. Experimental conditions were found where both filament stretch and relaxation produced reproducible results. Essentially Newtonian behaviour was found for both pure solvent and UV printing inks where a central droplet was formed by 'end pinching' near each drop reservoir after filament stretch. The addition of polymer resulted in an extended filament that broke at the central position with no subsequent drop formation.

Using an empirical correction factor, it was possible to obtain apparent extensional viscosities of fluids from mid-filament diameter profiles and where polymer was present, this value was found to depend on polymer concentration and Hencky strain. In the case of continuous inkjet (CIJ) inks, it was possible to make some correlation between the filament stretch in this paper and inkjet performance, however higher time and spatial resolution will be necessary to produce more definitive results. Matching filament stretching and thinning experiments with numerical simulation will also greatly help in differentiating between rheological, inertial and surface tension effects.

## Acknowledgements

This work was financially supported by the Engineering and Physical Science Research Council (EPSRC) and the Cambridge Inkjet Consortium (http://www.ifm.eng.cam.ac.uk/pp/inkjet/default.html). We are grateful to Domino and SunJet for kindly supplying the inks and Richard Marsden of Linx for allowing the use of their inkjet results. We would also like to acknowledge members of the inkjet consortium for valuable discussions on this subject.

## References

[1] B.J. de Gans, P.C. Duineveld, U.S. Schubert, Inkjet printing of polymers: state of the art and future developments, Adv. Mater. 16 (3) (2004) 203–213.
[2] A.L. Hudd, J.E. Fox, Recent advances in inkjet ink technologies, in Recent Progress in Ink Jet Technologies II, ISBN 0-89208-220-8, 1999, 424–429.
[3] G.H. McKinley, in The Korean Society of Rheology (Eds.), Recent developments in shear and extensional micro-rheometry of complex fluids, Proc. XIV$^{th}$ International Congress on Rheology, Seoul, Korea, ISBN 89-950057-5-0, 22-27 August, 2004, p. Re06-1-Re06-6.
[4] G.H. McKinley, in: D.M. Bindings, K. Walters (Eds.), Visco-Elastic-Capillary Thinning and Break-up of Complex Fluids, Rheology Reviews 2005, The British Society of Rheology, 2005, pp. 1–49.
[5] A.V. Bazilevsky, V.M. Entov, A.N. Rozkhov, in: D.R., Oliver, (Eds.), Third European Rheology Conference, Liquid Filament Microrheometer and Some of its Applications, Elsevier Applied Science, 1990, pp. 41–43.

[6] M.I. Kolte, P. Szabo, Capillary thinning of polymeric filaments, J. Rheol. 43 (3) (1999) 609–625.
[7] V.M. Entov, E.J. Hinch, Effect of a spectrum relaxation times on the capillary thinning of a filament elastic liquids, J. Non-Newtonian Fluid Mech. 72 (1997) 31–53.
[8] R.F. Liang, M.R. Mackley, Rheological characterisation of the time and strain dependence for polyisobutylene solutions, J. Non-Newtonian Fluid Mech. 52 (1994) 387–405.
[9] S.L. Anna, G.H. McKinley, Elasto-capillary thinning and breakup of model elastic liquids, J. Rheol. 45 (2001) 115–138.
[10] G.H. McKinley, A. Tripathi, How to extract the Newtonian viscosity from capillary breakup measurements in a filament Rheometer, J. Rheol. 44 (3) (2000) 653–670.
[11] M.R. Mackley, R.T.J. Marshall, J.B.A. Smeulders, The multipass rheometer, J. Rheol. 39 (6) (1995) 1293–1309.
[12] L.E. Rodd, T.P. Scott, J.J. Cooper-White, G.H. McKinley, Capillary breakup rheometry of low-viscosity elastic fluids, Appl. Rheol. 15 (2005) 12–27.
[13] V. Tirtaatmadja, G.H. McKinley, J.J. Cooper-White, Drop formation and breakup of low viscosity elastic fluids: effect of molecular weight and concentration, Phys. Fluids 18 (2006) 043101–043111.
[14] S. Berg, R. Kröger, H.J. Rath, Measurement of extensional viscosity by stretching large liquid bridges in microgravity, J. Non-Newtonian Fluid Mech. 55 (1994) 307–319.
[15] S. Gaudet, G.H. McKinley, H.A. Stone, Extensional deformation of Newtonian liquid bridges, Phys. Fluids 8 (10) (1996) 2568–2579.
[16] D.T. Papageorgiou, On the breakup of viscous liquid threads, Phys. Fluids 7 (1999) 1529–1544.
[17] M.P. Brenner, J.R. Lister, H.A. Stone, Pinching threads, singularities and the number 0.304, Phys. Fluids 8 (1996) 2827–2836.
[18] J. Eggers, Non linear dynamics and breakup of free surface flows, Rev. Mod. Phys. 69 (1997) 865–929.
[19] J. Eggers, Universal pinching of 3D axisymmetric free-surface flows, Phys. Rev. Lett. 71 (1993) 3458–3490.